Etchingless Microfabrication of a Thick Metal Oxide Film on a Flexible Polymer Substrate

Naoto Shirahata† and Atsushi Hozumi*,‡

International Center for Young Scientists (ICYS), National Institute for Materials Science (NIMS), 1-1 Namiki, Tsukuba, Ibaraki 305-0044, Japan, and National Institute of Advanced Industrial Science and Technology (AIST), 2266-98 Anagahora, Shimo-shidami, Moriyama-ku, Nagoya 463-8560, Japan.

Received June 21, 2004. Revised Manuscript Received October 11, 2004

Well-defined microstructures of metal oxide, i.e., tin oxide (SnO_x), were formed on a flexible polymer substrate from an aqueous solution of tin chloride without the use of any chemical or physical etching. First, through the chemical vapor deposition of tetraethoxysilane and subsequent photooxidation using 172 nm vacuum-ultraviolet (vacuum-UV) light, an extremely thin SiO_2 layer about 1 nm thick, which we call an "oxide nanoskin" (ONS), was formed on a polyimide (PI) substrate. Next, (heptadecafluoro-1,1,2,2-tetrahydrodecyl)trimethoxysilane (FAS) molecules were chemisorbed onto this ONS-covered PI (ONS/PI) surface from the vapor phase. As a control, a hydrophilized PI substrate was also treated under the same conditions. Both substrates were then photolithographically micropatterned using the same vacuum-UV light. Finally, the fabricated micropatterns composed of hydrophobic FAS- and hydrophilic SiOH-covered regions served respectively as chemically inert and active sites to provide a template for the area-selective deposition of SnO_x film. Although the SnO_x film was initially deposited on the entire substrate, the physisorbed film on the FAS-covered regions was easily eliminated from the surface by sonication in absolute toluene, while that on the SiOH-covered regions remained tightly adhered to the substrate surface. As confirmed by atomic force microscopy, square-shaped SnO_x micropatterns composed of $25 \times 25\ \mu m^2$ features were formed on the micropatterned FAS/ONS/PI substrates. However, on the substrate without the ONS layer, pattern resolution became significantly worse and elimination of the physisorbed SnO_x on the FAS-covered regions was incomplete. The ONS interlayer was effective both in forming a highly ordered FAS monolayer on the PI substrate and in obtaining excellent adhesion of the SnO_x film to the PI substrate. Furthermore, our process enabled us to control the thickness of the SnO_x microstructures within the range of a few hundreds nanometers to over 1 μm without distortion of their fine patterns. The SnO_x microstructures we obtained on the PI substrates were free of cracks or peeling even after thermal treatment and showed excellent mechanical properties.

1. Introduction

Recently, the microfabrication of electronic components onto various material surfaces, particularly onto polymeric surfaces, has been attracting more and more attention. Such microfabricated components are becoming increasingly important as both substrates and dielectrics for practical electronic applications, such as in flexible flat panels and wearable displays,[1,2] radio frequency identification tags,[3,4] electronic paper,[5] and biomedical microdevices,[6] due to their excellent properties including flexibility, light weight, ease of design and coloring, low cost, and good impact resistance. To fabricate such flexible microdevices, the ability to microprocess metal oxides is of particular importance, since metal oxides are key materials in microelectronics such as in high-*k* insulators[7] and phosphors[8] and in piezoelectric,[9] ferroelectric,[10] and ferromagnetic elements.[11] Unfortunately, due to their extremely high chemical durability and physical stability against electron beams and lasers,[12] metal oxides are difficult to micropattern with typical microfabrication processes employing chemical or physical etching. Thus, the microprocessing of metal oxides currently depends on photolithographic technology using resists. However, this technology is rather complicated since it consists of a sequence of many processes. The development of an effective etchingless microfabrication method for metal oxides is therefore highly sought after.

* To whom correspondence should be addressed. Telephone: +81-52-736-7175. Fax: +81-52-736-7182. E-mail: a.hozumi@aist.go.jp.
† ICYS, NIMS.
‡ AIST.

(1) Sirringhaus, H.; Tessler, N.; Friend, R. H. *Science* **1998**, *280*, 1741.
(2) Dodabalapur, A.; Bao, Z.; Makhija, A.; Laquindanum, J. G.; Raju, V. R.; Feng, Y.; Katz, H. E.; Rogers J. *Appl. Phys. Lett*. **1998**, *73*, 142.
(3) Ziemelis, K. *Nature* **1998**, *394*, 619.
(4) Brown, A. R.; Pomp, A.; Hart, C. M.; der Leeuw, D. M. *Science* **1995**, *270*, 972.
(5) Huitema, H. E. A.; Gelinck, G. H.; van der Puttern, J. B. P. H.; Kujik, K. E.; Hart, K. M.; Cantatore, E.; Herwig, P. T.; van Breemen, A. J. J. M.; der Leeuw, D. M. *Nature* **2001**, *414*, 599.
(6) Stieglitz, T. *Sens. Actuators* **2001**, *A90*, 203.
(7) Kingon, A. I.; Maria, J.-P.; Streiffer, S. K. *Nature* **2000**, *406*, 1032.
(8) Vayssieres, L.; Keis, K.; Lindquist, S.-E.; Hagfeldt, A. *J. Phys. Chem. B* **2001**, *105*, 3350.
(9) Martin, C. R.; Aksay, I. A. *J. Phys. Chem. B* **2003**, *107*, 4261.
(10) Gorbenko, O. Y.; Samoilenkov, S. V.; Graboy, I. E.; Kaul, A. R. *Chem. Mater.* **2002**, *14*, 4026.
(11) Cassassa, S.; Ferrari, A. M.; Busso, M.; Pisani, C. *J. Phys. Chem. B* **2002**, *106*, 12978.
(12) Takeda, S.; Ikuta, Y.; Hirano, M.; Hosono, M. *J. Mater. Res.* **2001**, *16*, 1003.

10.1021/cm0490165 CCC: $30.25 © 2005 American Chemical Society
Published on Web 12/07/2004

To overcome these obstacles, one promising strategy, which we call "monolayer template patterning" (MTP),[22] involves using micropatterned self-assembled monolayers (SAMs) as masks or templates. This approach is based on the site-selective deposition of metal oxides at low temperature from an aqueous media containing a precursor, taking advantage of the great difference in chemical reactivity between the monolayer-covered and -uncovered regions. Using this method, the microprocessing of metal oxides including TiO_2,[13] ZnO,[14] $SrTiO_3$,[15] Fe_3O_4,[16] La_2O_3,[17] Ta_2O_5,[18] and SnO_2[19] has been demonstrated. Although this process seems to meet the demands for metal oxide microfabrication, results have not yet been demonstrated on polymeric substrates for various reasons. When SAMs are directly fabricated on surface-activated polymer substrates, it is difficult for a well-ordered SAM to form, since the polar-functional groups formed on a polymer surface through surface modification methods using plasma or ultraviolet (UV) light are generally inhomogeneous and randomly distributed. Such a heterogeneous surface cannot provide adequate support for the preparation of a well-ordered SAM. Disordered SAMs are considered unfavorable as chemical templates for site-selective deposition. In addition, after a relatively short time, such functional moieties lose their polarity, resulting in a decrease of surface activity on the modified surface. Thus, it is difficult for covalent bonds to form between the metal oxide and the polymer surface, resulting in weak adhesion. Due to these serious shortcomings, MTP cannot be directly applied to polymer substrates. Furthermore, controlling thickness is crucial for the microprocessing of metal oxides based on MTP. It is common knowledge that the final performance of metal oxide films depends on their thickness. To obtain the best performance, it is frequently necessary to fabricate an oxide film more than 1 μm thick. It would however be unfavorable to deposit such a thick oxide film on polymeric materials, since the film would crack and/or peel due to the difference in thermal expansion coefficients. Finally, with MTP using an aqueous media, pattern resolution generally becomes significantly worse with increasing immersion time,[20] since the film grows not only on the predefined sites but also on undesired regions due to physisorption.[21] This has been the prime cause of difficulties using MPT to fabricate well-defined micropatterns of metal oxides with a thickness of more than 1 μm. To obtain clear-cut area selectivity, it has been necessary to strictly control the immersion time. In fact, one of the authors has recently reported that the area selectivity of such microstructures could be maintained when the thickness was controlled in the range of several nanometers to 100 nm.[22] To overcome these problems, an alternative method applicable to plastic substrates, which does not require precise thickness control, has been strongly needed.

In this article, we report on the fabrication of thick, clearly defined metal oxide microstructures strongly adhered to a flexible polymer substrate, that is, polyimide (PI), through a modified MTP. PI has been utilized mainly as a substrate for printed circuit boards due to its high heat resistance, mechanical strength, and insulating properties.[23,24] We selected tin oxide (SnO_x) as a model metal oxide, since it has been widely used as a gas-sensing material for sensor array systems and as a transparent conducting film for solar cells.[25−28] Prior to forming a SAM on the PI substrates, we fabricated a silicon dioxide (SiO_2) layer of molecular-scale thickness, i.e., an "oxide nanoskin" (ONS).[29] ONS-covered polymer surfaces have been reported to be almost identical to that of a Si substrate covered with native oxide (SiO_2/Si).[29] Accordingly, we expected that MTP could be similarly applied to an ONS-covered PI substrate. In this report, we focus on the effects of such an ONS interlayer on SAM formation and on the adhesion properties of SnO_x on polymer substrates both with and without the interlayer. Furthermore, we investigated the relation between the reaction time and the obtained microstructures, including their thickness, morphology, and spatial resolution. These are also compared with SnO_x microstructures formed on PI substrates without the ONS interlayer.

2. Experimental Section

2.1. Microfabrication of SnO_x Film. Microstructured SnO_x films were fabricated onto polymer substrates according to the process illustrated in Figure 1. In the first step seen in Figure 1a, 20 mm × 20 mm × 75 μm sample substrates cut from a commercial polyimide (PI) sheet (Dupont-Toray Co. Ltd., Kapton Super 300V) were photochemically hydrophilized. Hereafter, we refer to these samples as PI_{ox} substrates. Each sample was placed in a vacuum chamber evacuated by a rotary pump. The residual pressure in the chamber was maintained at about 10^3 Pa. The sample was then irradiated for 30 min with vacuum ultraviolet (vacuum-UV) light

(13) (a) Collins, R. J.; Shin, H.; De Guire M. R.; Heuer A. H.; Sukenik, C. N. *Appl. Phys. Lett*. **1996**, *69*, 860. (b) Masuda, Y.; Sugiyama, T.; Seo, W.-S.; Koumoto, K. *Chem. Mater*. **2003**, *15*, 2469. (c) Koumoto, K.; Seo, S.; Sugiyama, T.; Seo, W. S.; Dressick, W. J. *Chem. Mater.* **1999**, *11*, 2305. (d) Masuda, Y.; Sugiyama, T.; Koumoto, K. *J. Mater. Chem*. **2002**, *12*, 2643.
(14) Saito, N.; Ohashi, N.; Haneda, H. Koumoto, K. *Adv. Mater*. **2002**, *14*, 418.
(15) Gao, Y.; Masuda, Y.; Yonezawa, T.; Koumoto, K. *Chem. Mater*. **2002**, *14*, 5006.
(16) Nakanishi, T.; Masuda, Y.; Koumoto, K. *Chem. Mater*. **2004**, *16*, 3484.
(17) Gao, Y.; Masuda, Y.; Koumoto, K. *J. Colloid. Interface Sci*. **2004**, *274*, 392.
(18) (a) Clem, P. G.; Jeon, N.-L.; Nuzzo, R. G.; Payne, D. A. *J. Am. Ceram. Soc.* **1997**, *80*, 2821. (b) Masuda, Y.; Wakamatsu, S.; Koumoto, K. *J. Eur. Ceram. Soc*. **2004**, *24*, 301.
(19) (a) Bunker, B. C.; Pieke, P. C.; Tarasevich, B. J.; Campbell, A. A.; Fryxell, G. E.; Graff, G. L.; Song, L.; Liu, J.; Virden, J. W.; McVay, G. L. *Science* **1994**, *264*, 48. (b) Supothina, S.; De Guire M. R. *Thin Solid Films* **2000**, *371*, 1. (c) Shirahata, N.; Masuda, Y.; Yonezawa, T.; Koumoto, K. *J. Eur. Ceram. Soc*. **2004**, *24*, 427.
(20) (a) Pizem, H.; Sukenik, C. N.; Sampathkumaran, U.; McIlwain, A. K.; De Guire M. R. *Chem. Mater.* **2002**, *14*, 2476. (b) Shirahata, N.; Shin, W.; Murayama, N.; Koumoto, K. *J. Ceram. Soc. Jpn*. **2004**, *112*, S562.
(21) Shirahata, N.; Masuda, Y.; Yonezawa, T.; Koumoto, K. *Langmuir* **2002**, *18*, 10379.
(22) Shirahata, N.; Shin, W.; Murayama, N.; Hozumi, A.; Yokogawa, Y.; Kameyama, T.; Masuda, Y.; Koumoto, K. *Adv. Funct. Mater*. **2004**, *14*, 580.
(23) Gorman, B. P.; Anderson, H. U. *Thin Solid Films* **2004**, *457*, 258.
(24) Cho, N.-I.; Sul, Y. *Mater. Sci. Eng. B* **2000**, *72*, 184.
(25) Göpel, W.; Schierbaum, K. D. *Sens. Actuators* **1995**, *B26−27*, 1.
(26) Sharma, R. K.; Chan, P. C. H.; Tang, Z.; Yan, G.; Hsing, I.-M.; Sin, J. K. O. *Sens. Actuators* **2001**, *B72*, 160.
(27) Rakow, N. A.; Suslick, K. S. *Nature* **2000**, *406*, 710.
(28) Tsukuma, K.; Akiyama, T.; Imai, H. *J. Non-Cryst. Solids* **1997**, *210*, 48.
(29) Hozumi, A.; Masuda, T.; Sugimura, H.; Kameyama, T. *Langmuir* **2003**, *19*, 7573.

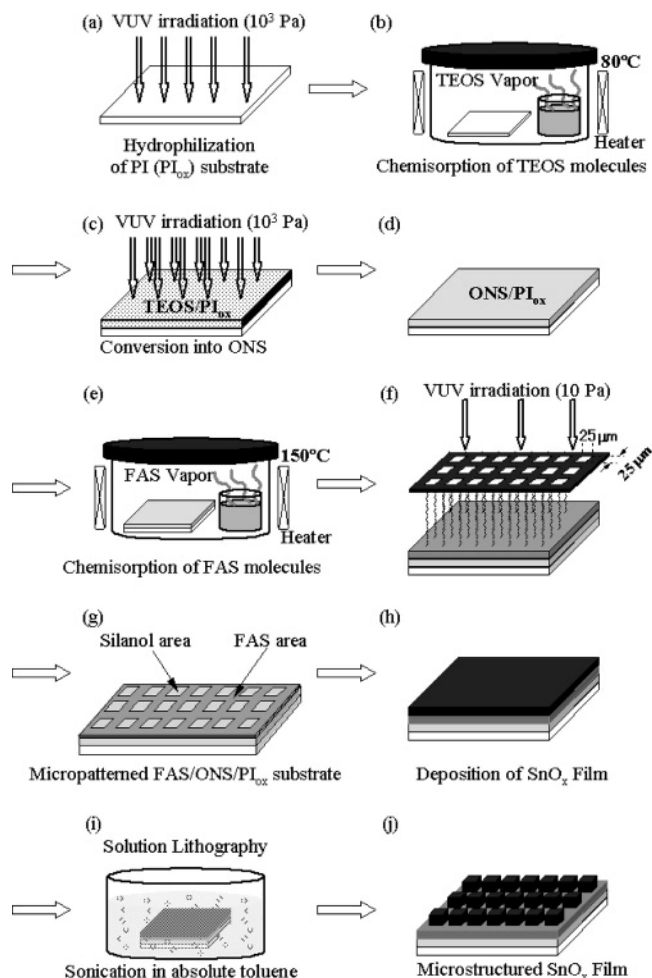

Figure 1. Schematic illustration of the microfabrication of metal oxide film onto the PI substrate.

generated from an excimer lamp (Ushio Inc., UER20-172V; λ = 172 nm and 10 mW/cm^2). The dose rate was about 18 J/cm^2. Due to this treatment, the PI surface became completely hydrophilic with its water-contact angle changing from about 71° to 5° or less. Next, tetraethoxysilane (TEOS; $Si[OC_2H_5]_4$; Wako Pure Chemical Industries, Ltd.) was adsorbed onto the PI_{ox} samples by chemical vapor deposition (CVD; Figure 1b). Each sample was placed together with a glass cup filled with 0.2 cm^3 TEOS into a 65 cm^3 Teflon container in a dry N_2 atmosphere with less than 10% relative humidity. The container was sealed with a cap and heated in an oven maintained at 80 °C for 3 h. Next, as seen in Figure 1c, to convert the chemisorbed TEOS molecules into an ultrathin silicon oxide layer, that is, an ONS, each of the samples was again irradiated for 30 min in a manner similar to the PI surface modification performed in the first step. Details of our ONS preparation method have been described elsewhere.[29−31] Following this, the ONS/PI substrate (Figure 1d) was chemically modified with an organosilane monolayer, as illustrated in Figure 1e. In a manner similar to the TEOS chemisorption in Figure 1b, an organosilane layer terminated with chemically inert functional groups, i.e., trifluorocarbon (CF_3) groups, was formed on the ONS/PI_{ox} surface by CVD using fluoroalkylsilane, that is, (heptadecafluoro-1,1,2,2-tetrahydrodecyl)trimethoxysilane (FAS; $CF_3[CF_2]_7$-$CH_2CH_2Si[OCH_3]_3$, Shin-Etsu Chemical Co., Ltd.; vapor pressure, 1 Torr at 86 °C) as a precursor.[32] The sample was treated at 150 °C for 3 h. To eliminate excess physisorbed FAS molecules, the sample was sonicated in absolute toluene for 30 min (not shown in Figure 1). As a control experiment, an FAS layer was also formed directly onto PI_{ox} substrates under identical conditions. Next, each sample was photolithographically micropatterned (Figure 1f). The sample was irradiated with vacuum-UV light for 30 min at a residual pressure of 10 Pa through a copper (Cu) mesh which square 25 × 25 μm^2 holes contacting its surface. A 10 mm thick quartz glass plate (Asahi Glass, synthetic silica glass AQX for Xe_2 172 nm excimer lamp) served as a weight on top of the mesh in order to attain satisfactory contact between the mesh and the sample surface. The transparency of the quartz plate at 172 nm was about 90%. The total light intensity at the surface was estimated to be about 9 mW/cm^2. The dose rate was about 16.2 J/cm^2. Finally, each of the patterned samples (Figure 1g) was immersed into a 1 M HCl solution containing 0.05 mol/L of $SnCl_2 \cdot 2H_2O$ and kept at 65 °C for 15−65 h (not shown in Figure 1). The pH value of this solution was about 1.2 and was kept constant during the reaction. After immersion, the substrate (Figure 1h) was immediately washed with Milli-Q water several times, blown dry with N_2 gas, and subsequently sonicated for 0.5−2.0 h in absolute toluene (Figure 1i). We have referred to this technique as "solution lithography".[22] This resulted in the formation of a microstructured SnO_x film (Figure 1j). Some of the samples were then heated at 300 °C for 3 h in ambient air.

2.2. Characterization. The thickness of the ONS on the PI_{ox} substrate was estimated from a cross-sectional image acquired by high-resolution transmission electron microscopy (HR-TEM, Hitachi, HF-2000). To reduce thermal damage to the sample, carbon thin film was first deposited on the PI substrate. The sample was then cut normal to its surface using a focused ion beam (Hitachi, FB-2000A) operated at 30 kV.

The static contact angles of three different liquids, i.e., water, methylene iodide and *n*-decane, were measured on the sample surfaces using a contact angle goniometer (Kyowa Interface Science, CA-X). Following the CVD treatment, these measurements were conducted on both FAS-covered samples without micropatterning. All contact angles were determined by averaging values measured at three different points on each sample's surface.

The surface energy of each sample was calculated using the following equation:[33]

$$\gamma_L(1 + \cos\theta_{SL}) = 2[(\gamma_s^{\,d}\gamma_L^{\,d})^{1/2} + (\gamma_s^{\,p}\gamma_L^{\,p})^{1/2} + (\gamma_s^{\,h}\gamma_L^{\,h})^{1/2}] \quad (1)$$

where γ_L is the liquid's surface energy and θ_{SL} is its contact angle on the solid surface. The superscripts d, p, and h indicate the dispersion, polar, and hydrogen bonding forces, respectively. Since the γ_L, $\gamma_L^{\,d}$, $\gamma_L^{\,p}$, and $\gamma_L^{\,h}$ values of the three liquids are known[34] (i.e., for water, γ_L = 72.8 mN/m, $\gamma_L^{\,d}$ = 29.1 mN/m, $\gamma_L^{\,p}$ = 1.3 mN/m, and $\gamma_L^{\,h}$ = 42.4 mN/m; for methylene iodide, γ_L = 50.8 mN/m, $\gamma_L^{\,d}$ = 46.8 mN/m, $\gamma_L^{\,p}$ = 4.0 mN/m, and $\gamma_L^{\,h}$ = 0 mN/m; and for *n*-decane, γ_L = 23.9 mN/m, $\gamma_L^{\,d}$ = 23.9 mN/m, $\gamma_L^{\,p}$ = 0 mN/m, and $\gamma_L^{\,h}$ = 0 mN/m), the surface energy (γ_S) of the sample was estimated to be the sum of the calculated $\gamma_s^{\,d}$, $\gamma_s^{\,p}$, and $\gamma_s^{\,h}$ values.

The ξ-potentials of the substrates were measured using an electrophoretic light scattering spectrophotometer (ELS-600, Otsuka Electronics). A quartz cell was used for measuring the electrophoretic mobility of polystyrene latex reference particles with an average diameter of 520 nm. The cell was filled with an appropriate

(30) Hozumi, A.; Wu, Y.; Hayashi, K.; Sugimura, H.; Takai, O.; Yokogawa, Y.; Kameyama, T. *Surf. Sci.* **2003**, *532−535*, 1056.
(31) Hozumi, A.; Inagaki, H.; Yokogawa, Y.; Kameyama, T. *Thin Solid Films* **2003**, *437*, 89.
(32) Hozumi, A.; Ushiyama, K.; Sugimura, H.; Takai, O. *Langmuir* **1999**, *15*, 7600.
(33) Hata, T. *Kobunshi* **1968**, *17*, 600.
(34) Kitazaki, Y.; Hata, T. *J. Adhes. Soc. Jpn. (1965−1989)* **1972**, *8*, 131.

amount of a solution of a certain pH containing the reference particles. An electric field of 80 kV was supplied between two Pt electrodes mounted at the both ends of the cell. A 1 mM KCl solution was used as a supporting electrode with its pH value arbitrarily adjusted over the range from 3 to 11 by adding HCl or NaOH. The ξ-potential was estimated from the average of 10 value measurements. The ξ-potential error was about $\pm$5 mV.

The micropatterns formed on the FAS/ONS/PI_{ox} and FAS/PI_{ox} substrates were observed at room temperature in ambient air by an atomic force microscope (AFM; Seiko Instruments Inc., SPA-300HV + SPI-3800N) in lateral force microscopic (LFM) mode using a Si probe (Seiko Instruments Inc., Cantilever; force constant = 0.12 N/m) covered with a native oxide layer. In addition, the surface topography of the deposits was acquired by the same AFM system in dynamic force microscopic (DFM) mode using another Si probe (Seiko Instruments Inc., Cantilever; force constant = 15 N/m) with a response frequency of 1 kHz. The scans were conducted at room temperature at 6.0×10^{-6} Pa.

Some of the samples were studied by X-ray photoelectron spectroscopy (XPS; Shimadzu, ESCA3400) using Mg Kα (E = 1253.6 eV) radiation. The binding energy (BE) scale was calibrated to provide $Au4f_{7/2}$ = 83.9 eV and $Cu2p_{3/2}$ = 932.8 eV. The X-ray source was operated at 10 mA and 12 kV. The core-level signals were obtained at a photoelectron takeoff angle of 90° (with respect to the sample surface). Data acquisition and processing were performed with a SUN Microsystems ULTRA 5 computer, using the VISION 2.0 processing package. The BE scales were referenced to 285.0 eV as determined by the locations of the maximum peaks on the C1s spectra of hydrocarbon (CH_x), associated with adventitious contamination. The accuracy of the BE determined with respect to this standard value was within $\pm$0.3 eV.

The crystal structure of the deposits before and after annealing was characterized by thin-film X-ray diffraction (XRD, MPX^3, MAC Science, Japan) with an incident angle of 5° using Cu Kα radiation with both a Ni filter and a graphite monochromator. Scanning speed was 1°/min over the range from 5 to 60°.

Adhesion strength of the patterned film was evaluated on the basis of a standard 3M Scotch-tape peeling test (Scotch tape no. 234; adhesive strength to steel 37 oz/in.). The microstructured film was firmly covered with the tape, and then the tape was quickly removed. The line edge acuity of the film was estimated in the same manner as described in ref 13c.

3. Results and Discussion

3.1. Formation of the FAS Layer. A typical cross-sectional HR-TEM image of a vacuum-UV-irradiated TEOS/PI_{ox} substrate is shown in Figure 2. As clearly indicated by the arrows, an extremely thin layer was found to have been formed on the PI_{ox} substrate. The actual thickness of this layer was estimated from this image to be only 1 nm or less. As confirmed by XPS, the BE of the Si2p spectrum for this vacuum-UV-irradiated TEOS/PI_{ox} substrate was located at 103.6 eV, the value of which is consistent with that of a Si substrate covered with native oxide (SiO_2/Si, 103.6 eV).[35] Therefore, an ONS undoubtedly formed on the PI_{ox} substrate, similar to those formed on polystyrene or poly(methyl methacrylate) substrates, as previously reported by one of the authors.[29−31] Due to this ONS coating, the surface chemical properties of the PI substrate were expected to be the same as those of SiO_2/Si substrates.[29,31]

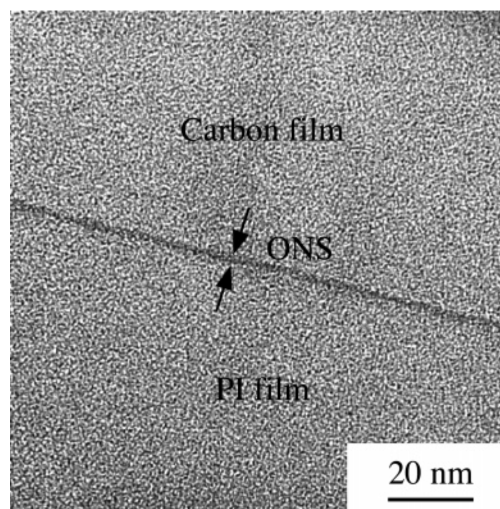

Figure 2. Cross-sectional HR-TEM image of an ONS on a PI substrate.

Table 1. Dispersive (γ_S^d), Polar (γ_S^p), and Hydrogen-Bonding (γ_S^h) Components of the Surface Energy (γ_S) for FAS/ONS/PI_{ox}, FAS/PI_{ox}, and FAS/SiO_2/Si Substrates[a]

	FAS/ONS/PI_{ox}	FAS/PI_{ox}	FAS/SiO_2/Si
	Contact Angle (deg)		
water	11.5	107	115
methylene iodide	92.3	74.0	95.7
n-decane	64.6	60.9	66.3
	Surface Energy (mN/m)		
γ_s^d	12.2	13.2	11.7
γ_s^p	0.1	14.2	0.1
γ_s^h	0.1	0.0	0.1
[b] γ_s	12.4	27.4	11.9

[a] All data were estimated from the static contact angles of water, methylene iodide, and *n*-decane on each substrate surface. [b] $\gamma_s = \gamma_s^d + \gamma_s^p + \gamma_s^h$.

As a result of the CVD treatment using the FAS precursor, both the ONS/PI_{ox} and PI_{ox} substrates (the latter serving as a control substrate) became hydrophobic. The resulting water-contact angles of the FAS/ONS/PI_{ox} and FAS/PI_{ox} substrates were about 115 and 107°, respectively, after removal of excessive physisorbed FAS molecules. This marked difference in the final water-contact angles observed between the FAS/ONS/PI_{ox} and FAS/PI_{ox} substrates was probably due to the difference in the density of the FAS molecules on the two substrate surfaces. As shown in Table 1, the γ_S value of the FAS/ONS/PI_{ox} substrate (12.4 mN/m) was almost consistent with that of a FAS/SiO_2/Si substrate (11.9 mN/m), and approximately one-half of that obtained for the FAS/PI_{ox} substrate (27.4 mN/m). As one of the authors has reported previously, chemisorbed FAS molecules on a SiO_2/Si substrate formed a 1.1 nm thick SAM in which the molecules were highly oriented with their CF_3 terminal groups aligned toward the outer surface.[32] Thus, in the case of our FAS/ONS/PI_{ox} sample, a highly oriented FAS-SAM is expected to have grown similarly on the ONS/PI_{ox} substrate. On the other hand, in the case of the PI_{ox} substrate, the density of the FAS molecules attached to the PI_{ox} surface was considerably lower than that of the other substrates. In particular, the γ_S^P value of the FAS/PI_{ox} substrate (14.2 mN/m) was much larger than those of the FAS/ONS/PI_{ox} (0.1 mN/m) and FAS/SiO_2/Si substrates (0.1 mN/m). This clearly demonstrates that the PI_{ox} surface underneath the FAS layer was

(35) Ouyang, M.; Yuan, C.; Muisener, R. J.; Boulares, A.; Koberstein, T. *Chem. Mater.* **2000**, *12*, 1591.

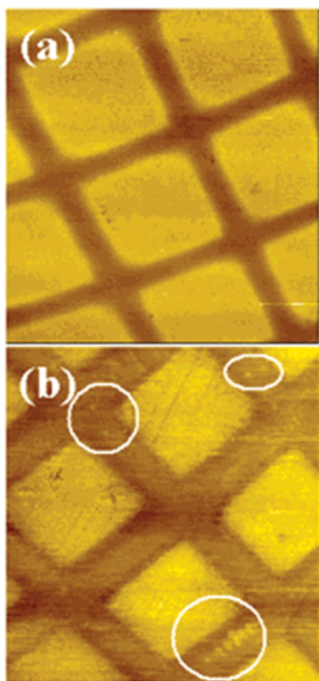

Figure 3. LFM images of micropatterned FAS template surfaces formed on (a) ONS/PI_{ox} and (b) PI_{ox} substrates by vacuum-UV irradiation for 30 min at 10 Pa through a copper mesh grid. The circles in b show brightly contrasted areas observed on the FAS-covered regions.

probably exposed to air to some extent. It can be concluded that the degree of surface coverage by the FAS molecules differed greatly between the ONS/PI_{ox} and PI_{ox} substrates. We will discuss this in more detail below.

3.2. Vacuum UV−Photopatterning of the FAS Layer. To fabricate a microtemplate for the area-selective deposition of SnO_x film, the FAS/ONS/PI_{ox} and FAS/PI_{ox} substrates were photolithographically micropatterned. Information on the chemical properties for both sample surfaces was obtained by LFM, as shown in Figure 3. The bright and dark areas in these images correspond to the photoirradiated and mesh-masked regions, respectively. As can be seen, square microstructures of $25 \times 25\ \mu m^2$ were clearly imaged through the friction force contrast between the vacuum-UV-irradiated and masked regions. The photoirradiated regions exhibited stronger friction force than the unirradiated FAS-covered regions. Due to the vacuum-UV irradiation, the FAS-SAM was decomposed and removed through the dissociative excitation of its organic components and subsequent oxidation with vacuum-UV-activated oxygen species.[36] In the vacuum-UV-irradiated regions, the bottom part of the FAS layer, which consisted of a 0.2−0.27 nm thick SiO_2 monolayer, remained on the substrate surface[37] due to vacuum-UV cleavage of the Si−C linkage in the molecules.[38] This vacuum-UV-irradiated FAS surface was highly hydrophilic with a water-contact angle of 5° or less and therefore adhered more strongly to the Si probe surface, which was also covered with a hydrophilic native SiO_2 layer. The friction force contrast on the vacuum-UV-irradiated regions was thus greater than that on the FAS-covered surface. However, compared to the image in Figure 3a, the friction force contrast in Figure 3b was relatively small. Moreover, several bright (hydrophilic) areas were observed even in unirradiated regions, as indicated by the circles. These are believed to have originated from incomplete termination with FAS molecules on the PI_{ox} substrate surface. As mentioned above, since the density of the FAS molecules is considered to have been low, a very small part of the hydrophilic PI_{ox} surface was probably exposed to air. In addition, the water-contact angle of the FAS/PI_{ox} surface was smaller than that of the FAS/ONS/PI_{ox} surface, indicating that the degree of coverage by FAS molecules on the former surface was lower than that on the latter.[39] Thus, it can be concluded that the FAS coverage on the PI_{ox} surface was probably lower than that on the ONS/PI_{ox} surface.

3.3. Formation of Microstructured Metal Oxide Film. Employing samples identical to those shown in Figure 3, we micropatterned metal oxide films. Although thin film initially formed uniformly over the entire surface of the samples, the physisorbed deposits on the FAS-covered regions, that is, the masked regions, were readily eliminated by solution lithography with absolute toluene. Thin-film XRD of the deposited film detected three broad peaks at $2\theta = 26.6°, 33.9°$, and 51.8° corresponding respectively to the (100), (101), and (211) planes of the cassiterite phase (JCPDS 41-1445). This XRD pattern indicates that the film was composed of a single cassiterite phase without a secondary phase of SnO. The stoichiometry of the deposited SnO_x film was estimated by XPS to be in the range of $2 < x < 3$. Typical optical micrographs of the SnO_x films deposited on both the micropatterned FAS/ONS/PI_{ox} and FAS/PI_{ox} substrates (deposition time of 24 h; sonication time of 2 h) are shown in Figure 4a,b, respectively. As can be seen in Figure 4a, SnO_x deposits with continuous filmlike features remained on the photoirradiated regions, while the surrounding regions, which had not been photoirradiated and were thus FAS-covered, were free of deposits. To investigate the adherent properties of the microfabricated SnO_x films on the photoirradiated regions, we performed a 3M Scotch-tape peeling test. The micropatterned SnO_x films did not peel off with the tape, and their resolution remained almost intact even after the test as evidenced by AFM (image not shown). These results clearly indicate that the deposits grown on the vacuum-UV-irradiated regions stayed tightly fixed to the surface, while the deposits on the FAS-covered regions had been completely eliminated. On the other hand, no microstructured features could be seen on the micropatterned FAS/PI_{ox} substrate shown in Figure 4b. Both sample surfaces were observed in detail by DFM. As clearly seen in the DFM image in Figure 4c, highly resolved micropatterns composed of SnO_x film grew site-selectively on the photoirradiated regions of the micropatterned FAS/ONS/PI_{ox} substrate. In contrast, it was difficult to achieve clear micropatterns on the FAS/PI_{ox} substrate, as shown by Figure 4d. This sample had been treated in absolute toluene for 30 min. As can be clearly seen, the SnO_x remained deposited relatively evenly

(36) Sugimura, H.; Ushiyama, K.; Hozumi, A.; Takai, O. *Langmuir* **2000**, *16*, 885.
(37) Brunner, H.; Vallant, T.; Mayer, U.; Hoffman, H. *Langmuir* **1996**, *12*, 4614.
(38) Dulcey, C. S.; Georger, J. H.; Krauthamer, J. V.; Stenger, D. A.; Fare, T. L.; Calvert, J. M.; *Science* **1991** *252*, 551.
(39) Choi, S.-H.; Newby, B. Z. *Langmuir* **2003**, *19*, 1419.

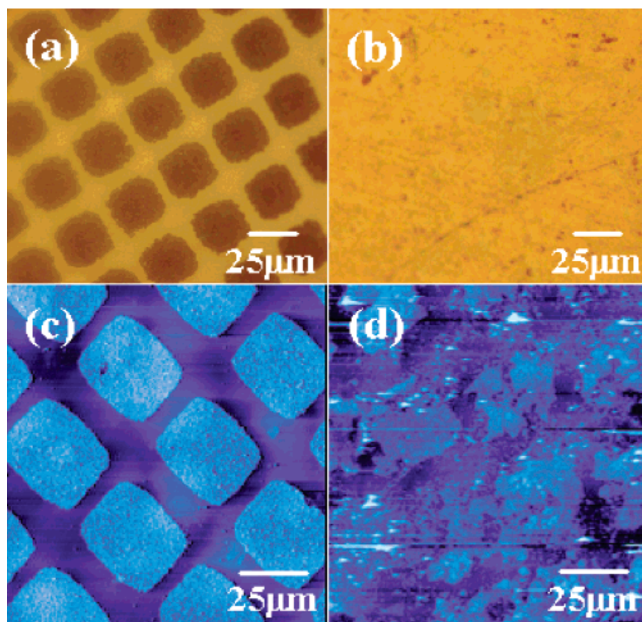

Figure 4. Optical micrographs (a and b) and DFM images (c and d) of microstructured SnO_x film fabricated on two different substrates. Panels a and c show SnO_x film deposited on a microstructured FAS/ONS/PI_{ox} substrate, while b and d show SnO_x film deposited on a microstructured FAS/PI_{ox} substrate. Both films were obtained by immersion the samples for 24 h in 1 M HCl solution containing 0.05 mol/L $SnCl_2 \cdot 2H_2O$ kept at 65 °C. All images were acquired after sonication with absolute toluene for 2 h (a−c) or 30 min (d).

on the FAS-covered regions, and there was marked distortion of the deposits on the vacuum-UV-irradiated regions. When sonication was prolonged up to 2 h (image not shown), the micropattern became hardly recognizable by DFM. However, residual deposits were observed over the entire sample surface, indicating that they still remained not only on the vacuum-UV-irradiated regions, but also on the FAS-covered regions. This clearly reveals that the FAS-covered regions did not effectively serve as a mask to prevent SnO_x deposition. Moreover, adhesion of the deposits to the vacuum-UV-irradiated regions was insufficient. We believe that this significant difference between the samples in the features of the final pattern must be related to the density of the FAS molecules on both surfaces. We therefore investigated the surface chemical properties at the vacuum-UV-irradiated and unirradiated regions on both samples. However, since it was difficult to determine the actual surface properties of the vacuum-UV-irradiated and unirradiated regions selectively, we characterized both FAS/ONS/PI_{ox} and FAS/PI_{ox} substrates before and after vacuum-UV irradiation without micropatterning.

Figure 5 shows the variation in the ζ-potential with the pH for vacuum-UV-irradiated FAS/ONS/ PI_{ox} and FAS/PI_{ox} substrates (indicated by the open and solid circles, respectively). As a control experiment, observations of a SiO_2/Si substrate were also performed in the same manner (indicated by the solid triangles). Over the range from pH 3 to 11, the SiO_2/Si surface showed negative ζ-potentials from ca. −22 to −82 mV due to the partial ionization of surface silanol (Si−OH) groups.[40] The isoelectric point (IEP) of this surface

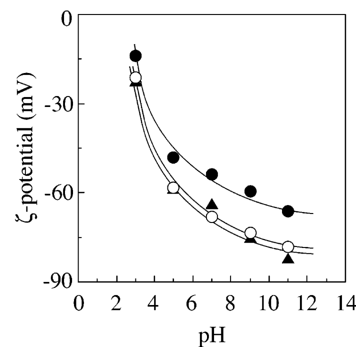

Figure 5. Comparison of ζ-potentials as a function of pH for an irradiated-FAS/ONS/PI_{ox} substrate (open circles), an irradiated-FAS/PI_{ox} substrate (solid circles), and a SiO_2/Si substrate (solid triangles).

was estimated to be at pH 2.0. It is noteworthy that the ζ-potential vs pH curves for the vacuum-UV-irradiated FAS/ONS/PI_{ox} and SiO_2/Si substrates are nearly identical in shape and magnitude over the entire pH range. Thus, we concluded that the vacuum-UV-irradiated FAS/ONS/PI_{ox} surface showed chemical properties very similar to the SiO_2/Si substrate and that the oxide layers (i.e., SiO_2 monolayer and ONS) had covered the PI substrate almost completely. On the other hand, the vacuum-UV-irradiated FAS/PI_{ox} surface was found to be 15−39% less charged than the vacuum-UV-irradiated FAS/ONS/PI_{ox} and SiO_2/Si substrates. In addition, the IEP of this sample, observed to be around pH 3.5, was higher than those of the vacuum-UV-irradiated FAS/ONS/PI_{ox} and SiO_2/Si substrates. This clearly indicates that the FAS molecules insufficiently covered the PI_{ox} surface. Since, as mentioned above, the density of the FAS monolayer on the PI_{ox} surface was considerably lower, the molecules at the bottom of the FAS comprising the SiO_2 monolayer were loosely packed. This marked difference in surface properties must account for both the final morphology and the adhesion properties of the deposits on the vacuum-UV-irradiated regions.

As a result of hydrolysis, the $SnCl_2$ precursors formed fine particles in the solution with a chemical composition of $SnO_{2-x/2-y/2}(OH)_xCl_y$.[22] These particles readily anchored to the irradiated-FAS on the ONS interlayer through a covalent bond (i.e., a Sn−O−Si bond) formed by the dehydration reaction between the hydroxyl groups of the partially hydrolyzed Sn precursors (Sn−OH) and silanol (Si−OH) groups on the SiO_2 monolayer.[22] Since the surface properties of the vacuum-UV-irradiated regions on the micropatterned FAS/ONS/PI_{ox} substrate were found to be almost identical to those of the SiO_2/Si substrate, as shown in Figure 5, the SnO_x deposits on these regions were strongly attached to the surface through the Sn−O−Si bonds. Thus, these deposits kept their fine microstructures even after sonication for 2 h. In contrast, in the case of PI_{ox} substrate, since the SiO_2 monolayer insufficiently covered the vacuum-UV-irradiated regions, adhesion between the deposits and the SiO_2 monolayer surface was incomplete, resulting in their incomplete elimination.

It is crucial to elucidate the properties of the FAS-covered surfaces, since they also affect the elimination efficiency of

(40) Hozumi, A.; Sugimura, H.; Yokogawa, Y.; Kameyama, T.; Takai, O. *J. Colloid. Interface Sci.* **2001**, *182*, 257.

(41) Gawalt, E. S.; Avaltroni, M. J.; Koch, N.; Schwartz, J. *Langmuir* **2001**, *17*, 5736.

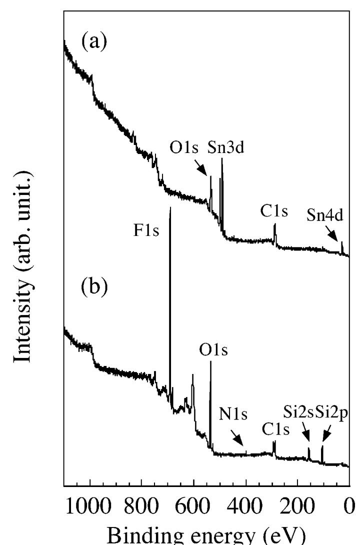

Figure 6. XPS spectra of (a) ONS/PI_{ox} and (b) $FAS/ONS/PI_{ox}$ substrates covered with SnO_x film after sonication for 2 h in absolute toluene. The film deposition time was 65 h for each sample.

the deposits by sonication. When the deposits on the FAS/ ONS/PI_{ox} substrate were sonicated for 2 h in toluene, the root-mean-square roughness (R_{rms}) and water-contact angle of the surface changed from 86.2 nm and 52° to 1.78 nm and 115°, respectively, which are consistent with those of the initial $FAS/ONS/PI_{ox}$ surface (R_{rms} = 1.86 nm and water-contact angle of 115°). Thus, physisorbed SnO_x deposits are considered to have been removed by the sonication. This is also supported by our XPS results shown in Figure 6. Comparing the spectra of the ONS/PI_{ox} and the FAS/ONS/ PI_{ox} substrates, indicated by a and b, respectively, the peaks referring to both Sn3d and Sn4d disappeared completely from the $FAS/ONS/PI_{ox}$ substrate spectrum after sonication. We therefore conclude that the $FAS/ONS/PI_{ox}$ areas served effectively as a mask to prevent the immobilization of SnO_x through the Sn−O−Si covalent linkage mentioned above, although SnO_x deposits initially physisorbed onto the surface. On the contrary, in the case of the PI_{ox} substrate, since the FAS molecules were packed loosely, their masking ability was inferior to that of the FAS on the ONS/PI_{ox} substrate, resulting in incomplete elimination of the deposits from the FAS-covered surface even after sonication. This is also supported by our surface energy data and LFM images described above.

Finally, we investigated the influence of the reaction time on the thickness, area selectivity, and resolution of the SnO_x films on the micropatterned $FAS/ONS/PI_{ox}$ substrates.

Parts a and b of Figure 7 show DFM images of microstructured SnO_x films prepared for 15 and 65 h, respectively. As can be seen, well-defined microstructures composed of 25 × 25 μm^2 square-shaped features were clearly imaged for both samples. It is noteworthy that by varying the reaction time the thickness of the patterned SnO_x film was controllable over the range of tens of nanometers to over 1 μm. Although the thickness of the sample shown in Figure 7b was more than 1 μm, no cracks or exfoliation were detectable. Indeed, as can be seen in Figure 8, the sample consisting of micropatterned (identical to Figure 7b) and unmicropatterned regions appeared to have excellent mechanical flexibility even after thermal treatment. Furthermore, the DFM images in Figure 7 demonstrate that while the thickness of the SnO_x film varied greatly according to the reaction time, its area selectivity was less dependent. This is a clear advantage offered by our process, since the site selectivity of deposits on a micropatterned template have generally become worse with an increase in immersion time due to physisorption of deposits on undesired areas.[20,21] To obtain the best possible area selectivity, various film growth conditions, including reaction time, temperature, concentration, and surrounding atmosphere, have been precisely regulated.[21] However, since our technique enables the complete elimination of undesired deposits, a relatively thick micropatterned SnO_x film with excellent site selectivity can be fabricated without the need for any additional precise reaction control. Moreover, the edge features of our patterned films were relatively sharp. For precise evaluation, we estimated the variation in the nominal pattern width based on the method described in ref 13c. By employing the two-dimensional AFM image of the microppattern shown in Figure 4c, we measured the pattern

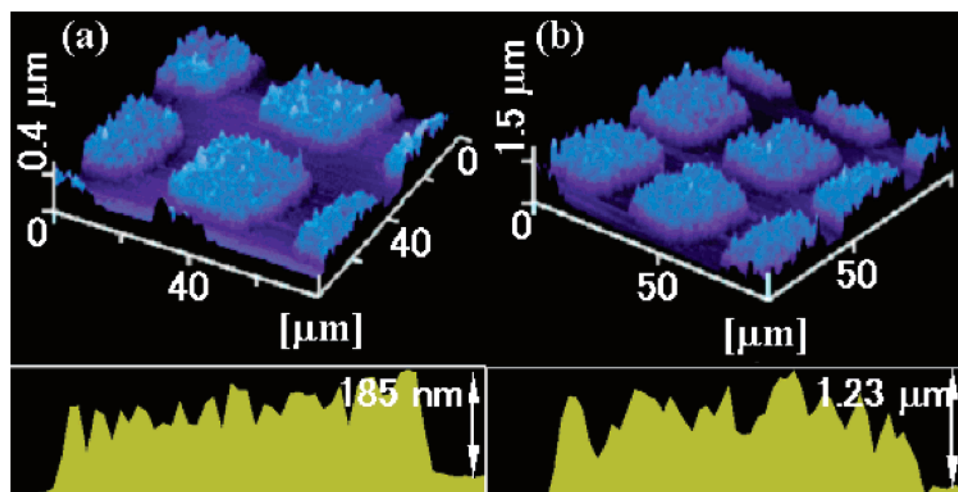

Figure 7. DFM images and their corresponding cross-sectional images of microfabricated SnO_x films with different thicknesses on an ONS/PI_{ox} substrate covered with an FAS template. Film depositions were conducted at 65 °C for (a) 15 or (b) 65 h in a 1 M HCl solution containing 0.05 mol/L $SnCl_2 \cdot 2H_2O$. The sonication time for both samples was 2 h.

Figure 8. Photograph of a sample identical to Figure 7b, demonstrating excellent mechanical flexibility even after thermal treatment. The sample was heated at 300 °C for 3 h under ambient air.

width at 15 equally spaced points on each square pattern in the image. The average width of each square pattern in this image is about 24.2 μm. The pattern edge roughness, as measured by the standard variation of the line width, is about 1.2 μm. Thus, the variation in the nominal pattern width was calculated to be about 5% (i.e., 1.2/24.2 × 100), which meets the specifications demanded for current electronics design.[13d] These results demonstrate that, by our technique presented here, we were able to fabricate well-defined micropatterned SnO_x film over 1 μm in thickness on a polymer substrate without either cracking or peeling.

4. Conclusion

We have developed an etchingless technique for the fabrication of metal oxide, i.e., SnO_x, microstructures on a flexible polymer substrate from an aqueous solution of tin chloride. A micropatterned FAS layer was photolithographically prepared on PI substrates both with and without an ONS interlayer to create a substrate surface composed of two distinct types of regions: one with a hydrophilic SiOH surface (vacuum-UV-irradiated regions), and the other with a hydrophobic surface covered with FAS molecules (unirradiated regions). This micropattern was used as a template for the microfabrication of SnO_x film, in which the SiOH- and FAS-covered surfaces served respectively as chemically active and inert sites for SnO_x deposition. Although SnO_x film was initially deposited over the entire sample surface, the deposits on the FAS-covered regions could be eliminated selectively by sonication in absolute toluene. As a result, well-defined micropatterns of SnO_x film composed of 25 × 25 μm^2 square-shaped features were formed on the PI substrates. However, we found that the final morphology and pattern resolution of the SnO_x microstructures depended significantly on the quality of the FAS layer. When the PI_{ox} surface was covered with an ONS, a highly ordered FAS-SAM formed on the ONS/PI_{ox} substrate, similar to that formed on a SiO_2/Si substrate, as confirmed by contact-angle analysis. Furthermore, as evidenced by ζ-potential measurements, the surface acidity of the vacuum-UV-irradiated FAS/ONS/PI_{ox} sample was identical to that of the SiO_2/Si substrate. Consequently, in the case of the micropatterned FAS/ONS/PI_{ox} substrate, the SnO_x film deposited on the vacuum-UV-irradiated regions, i.e., the SiOH surface, adhered very strongly to the surface through Si−O−Sn bonds, while the deposits on the unirradiated regions, i.e., the FAS-SAM-covered surface, were completely removed by sonication, as confirmed by XPS. In contrast, it was difficult to achieve well-shaped SnO_x microstructures on the micropatterned FAS/PI_{ox} substrate without the ONS interlayer, due to insufficient surface coverage by FAS molecules. Filmlike features still remained on the FAS-covered regions even after sonication. The ζ-potential measurements clearly demonstrated that the vacuum-UV-irradiated regions of the FAS/PI_{ox} substrate were insufficiently covered with SiOH groups. Thus, the SnO_x film deposited on the vacuum-UV-irradiated regions was mostly exfoliated due to sonication. Consequently, pattern resolution and morphology were significantly worse compared to those for the micropatterned FAS/ONS/PI_{ox} substrate. Our experimental results offer clear proof that the ONS interlayer on the PI surface was crucial for both the formation of the FAS-SAM and the microfabrication of a metal oxide film on the polymer substrate.

Our technique, demonstrated here, offers a further advantage in that by selecting an appropriate deposition time the microstructures' thickness can be freely controlled over the range of several tens of nanometers to over 1 μm without any marked change in either morphology or resolution. This is in marked contrast to previous results obtained with liquid-phase processes, where the target materials generally deposited not only on the predefined regions but also on undesired regions with increasing immersion time, resulting in decreased pattern resolution.[20,21] In such cases, film thickness had to be strictly regulated to ensure area selectivity. However, our solution lithography technique allows the complete elimination of the physisorbed deposits on the undesired regions. Thus, precise thickness control is not absolutely necessary. Moreover, despite having greater thickness, that is, more than 1 μm, our resulting samples were free of cracks or peeling even after thermal treatment and showed excellent mechanical properties.

By selecting an appropriate precursor solution, our microfabrication method demonstrated here can be applied to various metal oxides other than SnO_x. Thus, we believe our technique to be readily and widely applicable to the production of novel polymer-based flexible microsensors and other devices using metal oxides.

Acknowledgment. The authors would like to express their gratitude to Prof. Kunihito Koumoto, Dr. Yoshitake Masuda, and Mr. Tsuyoshi Nakanishi for SPM usage.

CM0490165